ADVANCES in NATURAL and APPLIED SCIENCES

ISSN: 1995-0772
EISSN: 1998-1090
2017 February 11(2): pages 85-93

Published BY**AENSI Publication**
http://www.aensiweb.com/ANAS
Open Access Journal

Prediction of Effective Thermal Conductivity in Light Brick-Autoclaved Aerated Concrete With the material Additive Composition Variations Using Artificial Neural Network Approach

[1]Zulkifli, [2]Detak Yan Pratama, [3]Dyah Sawitri, [4]Ali Musyafa

[1,2,3,4]Department of Engineering Physics, Faculty of Industrial Technology, Sepuluh Nopember Institute Of Technology, Surabaya, INDONESIA

Received 18 December 2016; Accepted 12 February 2017; Available online 20 February 2017

Address For Correspondence:
Ali Musyafa', Department of Engineering Physics, Faculty of Industrial Technology, Sepuluh Nopember Institute Of Technology, Kampus ITS Keputih, Sukolilo, Surabaya 60111
E-mail: musyafa@ep.its.ac.id,

ABSTRACT

Indonesia with raw material limestone abundant, light brick AAC is the most important component in the construction of buildings, so that needs light brick AAC qualified in mechanical and thermal properties of acoustic. In the research domain lightweight brick lifting who qualified thermal conductivity properties. Advantages of light brick AAC low density of about 500 to 650 kg/m^3, more economical, suitable for multi-storey buildings can reduce the weight of 30 to 40 % compared with conventional brick (clay brick) The research of thermal conductivity prediction of Autoclaved Aerated Concrete (AAC) has been completed by using Neural Network (NN). Main chemical compositions of AAC in this research were 20 – 45% wt Oxygen (O), 25 – 30 wt % Silicon (Si) and 20 – 40%wt Calcium (Ca). Besides, the density and additive components such as Aluminum (Al), Sulfur (S) and Magnesium (Mg) became important factors which could influence thermal conductivity of AAC. The addition of these components to the main component was accomplished by using back propagation NN. Main chemical composition, the additive component and density were as the input of NN and thermal conductivity as its output. One hidden layer was located between input and output which had 1 to 10 hidden nodes. The data were trained through NN by applying Lavenberg Marquardt as training algorithm. The best performance of the network was achieved when the average MSE result in validation part was 0,003269. This result occurred if there were 3 hidden nodes in hidden layer. The valid network could be used to predict thermal conductivity of four AAC samples; i.e. AAC-1, AAC-2, AAC-3, AAC-4. Predicted thermal conductivity of ACC gave the following results: AAC-1 = 0.243 W/mK, AAC-2 = 0.29 W/mK. AAC-3 = 0.32 W/mK AAC-4 = 0.32 W/mK. Also, it was found that thermal conductivity was rising along with the increasing of Si concentration and density. Otherwise, the increasing Al concentration would reduce the thermal conductivity and AAC low density.

KEYWORDS: Back propagation neural network, autoclaved aerated concrete, thermal conductivity

INTRODUCTION

Energy consumption of a building is affected by various factors, one of which relates to the thermal insulation properties of materials being used. Materials with good thermal insulation properties are able to reduce electrical energy consumption for cooling needs of a building. Autoclaved aerated concrete (AAC) of thermal conductivity should be in the range of 0.24 – 0.32 W/m.K is a kind of material that is currently widely

ToCite ThisArticle: Zulkifli, Detak Yan Pratama, Dyah Sawitri, Ali Musyafa., Prediction of Effective Thermal Conductivity in Light Brick-Autoclaved Aerated Concrete With the material Additive Composition Variations Using Artificial Neural Network Approach. **Advances in Natural and Applied Sciences**. 11(2);Pages: 85-93

used for its excellent thermal insulation properties. In the research domain lightweight brick lifting who qualified thermal conductivity properties. Advantages of light brick AAC low density of about 500 to 650 kg/m^3. AACs are incorporating porous structure so that it has a lower density and better thermal insulation capabilities than conventional brick, and AAC processing in *autoclave* at temperature 180-190 ^oC.

Thermal insulation properties of any materials, including AAC are determined by the thermal conductivity. Materials with lower thermal conductivity coefficient give better thermal insulation capability. In case of AAC, factors that affect the thermal conductivity are as follow: density, moisture content, temperature, porosity and mineral composition [1-5]. For determine the maximum amount of Si in AAC, can calculate the value of Vf represents volume fraction of air in AAC, the amount of Si in AAC should be no greater than 26.57%wt, since the value of Vf will be negative if Si amount exceed this value. Thermal Conductivity of AAC, mineral quart 7,2 – 13,6 W/m.K and mineral tobermorite 0,18 – 0,2 W/m.K. The elemental composition of AAC sampel, dominant unsure O (29-45 % wt), Si (25-30 %wt) and Ca (20 – 40 %wt), additive unsure Al (1- 7 %wt)

Artificial Neural Network (ANN) or Neural Network is an information processing system with ability to learn, remember, and resolve the problem based on learning (training) 1 to 10 hidden nodes and 85% of total 18 data pair were used for training, while the remaining 15% were used for validation. ANN has been widely used in various recearch to predict properties of materials including: the thermal and mechanical properties [4-7]. In this recearch, Artificial Neural Networks Back propagation is used to predict thermal conductivity of four types AAC sample based on compositional variation of Si, and Ca.

MATERIALS AND METHODS

In this recearch, there were two types of data, i.e. secondary data for training purposes and primary data that were used to test the network. 18 data pairs that contained input and target were obtained from 3 three research papers [8-10]. Summary of input data and the target can be seen in Table 1 and Table 2 below.

Table 1: Input Data (training)

Variable	N*	Max	Min	Mean	St.dev
Si	18	32,56	12,18	20,67	6,93
Ca	18	31,96	18,3	23,69	3,51
Al	18	6,67	1,11	4,09	2,22
O	18	46,28	38,87	41,66	1,86
ρ*	18	1219	504	712	180,13

*ρ – density; *N – number of data

Table 2: Target Data (training)

Variable	N*	Max	Min	Mean	St.dev
λ*	18	0,376	0,123	0,23	0,09

* λ – density; *N – number of data

In contrast to the secondary data, primary data for testing the network were obtained from thermal conductivity measurement of four AAC sample (shown in figure 1) Grutzeck, M., (2005).

Fig. 1: Four AAC samples

Density measurement, EDX, and thermal conductivity measuremnt were carried out on the 4 AAC samples. Summary of the test input data can shown in Table 3. Lee,J., and C. B. S. (2012).

Table 3: Summary of test input data

Unsure Variable	N*	Max	Min	Mean	St.dev
Si	4	5,56	27,37	17,24	11,02
Ca	4	29,62	51,5	40,43	11,87

Al	4	0	1,69	0,84	0,97
O	4	38,71	41,8	40,12	1,61
ρ*	4	509	632	585	53,33

*ρ –density; *N – number of data

Neural Network, Neural Network Toolbox in Matlab provides various functions for creating and developing the neural network. The neural networks were designed through the following steps:

- Load the data (Input and Target)
- Normalized Data Input and Target into the range of 1 and -1.

The data are normalized according to the equation 3:

$$y = \frac{2(x - x_{min})}{x_{max} - x_{min}} - 1 \quad (1)$$

Where :
x = initial value
y = normalized value
x_{max} = maximum value
x_{min} = minimum value

- Initialize activation function (tansig and purelin)
- Specified training parameter (three important parameters to be specified are epochs = 100; training goal = 1e-5; validation checks = 10, while the remaining parameter were left unchanged)
- Initialize weight and bias
- Start training
- Store the Network

In this research, we trained 10 neural network that varries in the number of hidden node i.e. 1 to 10 hidden nodes. Each configuration was trained 3 times with Levenberg-Marquardt backpropagation algorithm. As a result, we have 30 networks with different weigh and biases. In this research, 85% of total 18 data pair were used for training, while the remaining 15% were used for validation. Neural Network architecture that is employed in this study was shown in Figure 2. Siang, J., (2009).

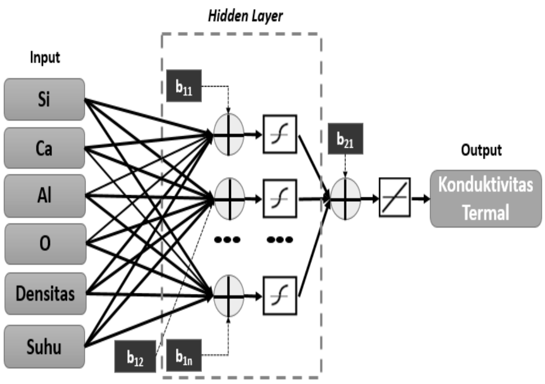

Fig. 2: Backpropagation Neual Network (NN) architecture

Evaluating the Networks:

The best network among the 30 models of neural network with 10 different hidden node situated on the MSE (Mean Squared Error) Average validate each of the NN. Mean Square Error (MSE) expressed by the equation:

$$MSE = \frac{1}{N}\sum_{i=1}^{N}(T_i - Y_i)^2 \quad (2)$$

where :
N = number of data

T_i = target value
Y_i = output value

Testing Using the network (NN), The network that was used in the testing phase is the one that has been selected. First thing done before the test is to call the data and load it into the Mat lab workspace. Next will be compared to the value of the Target and the output of ANN, which together form the thermal conductivity of lightweight brick

Effect of Composition Variation on Thermal Conductivity of AAC, Si, Ca and Al are the main elements that influence the formation of a dominant phase contained in the lightweight brick that is calcium silicate hydrate. Narayanan, N. and K. Ramamurthy,(2000). The influence of the variation of composition of these elements to the thermal conductivity can be determined by performing simulations using a neural network in which one element is varied in value while other variables constant value. Limitation value of the composition of an element contained in the light brick can be searched using the following equation:

$$Vf = \frac{\lambda_f(\lambda_m - \lambda)}{\lambda(\lambda_m - \lambda_f)} \quad (3)$$

Where:
Vf =
Volume fraction of air in AAC
λ =
λ_f = Thermal conductivity (simulation result)
Thermal conductivity of air in atmospheric pressure and T = 300K (0,026 W/mK) [11]
λ_m = Thermal conductivity of *tobermorite* (0,2 W/mK) [12]

RESULTS AND DISCUSSION

Composition of AAC, Table 5 below shows the elemental composition of AAC (AAC-1, AAC-2, AAC-3 and AAC-4). High concentration of calcium and oxygen as well as the presence of sulfur in the whole AAC sample indicates that the area on the surface of the test had undergone carbonation due to environmental exposure. Carbonation is a major degradation in AAC that occurs when Ca $(OH)_2$ and C-S-H phase in AAC react with CO_2 in the air to form $CaCO_3$. Further degradation may occur when $CaCO_3$ react with sulfuric acid in the air and produce gypsum. This is the mechanism behind the presence of sulfur in the 4 AAC samples [13].

Table 5: Elemental composition of AAC sample

Sample	Composition (wt%) average					
	Si	Ca	Al	O	Mg	S
AAC-1	27,37	30,74	1,67	38,79	0,61	0,83
AAC-2	23,89	29,62	1,69	41,19	0,61	1,00
AAC-3	5,56	51,50	0	41,80	0	1,14
AAC-4	1,26	49,88	0	38,71	0	1,26

Training and Evaluation result:

Table 6 below shows average MSE value for training and validation of 10 network model with variation in hidden nodes. It was found that network with three hidden node produce average MSE of 0.003269

Table 6: Mean Square Error (MSE) comparison for each network

Number of Hidden Node	MSE (Average)	
	Training	Validation
1	0,002855	0,005908
2	0,002668	0,005516
3	0,002434	0,003269 *)
4	0,004751	0,003833
5	0,002383	0,006464
6	0,002625	0,007059
7	0,002716	0,008955
8	0,00225	0,003891
9	0,002897	0,008206
10	0,002974	0,004768

*) Optimum product

Table 7. shows comparison between the MSE validation values for 3 networks, each with 3 hidden nodes this has been trained with different initial weights. It is found that the network named, NN-2 produces MSE validation of 0.002252.

Table 7: Comparison Mean Square Error (MSE) Validation JST with one hidden node for Three times of training

Name of Neural Network	Mean Square Error (MSE) *Training*	Mean Square Error (MSE) Validation
NN-1	0,002694	0,003716
NN-2	0,002763	0,002252 *)
NN-3	0,001845	0,00384

*) Optimum product

Comparison between MSE training and validation NN-2 is shown in Figure 3. It appears that the best validation performance or in other words MSE validation achieve minium value in the epoch-11. In the next epoch, it appears that MSE validation rise until the end of training stop on the epoch of the 21st, Zulkifli, et.al. (2015).

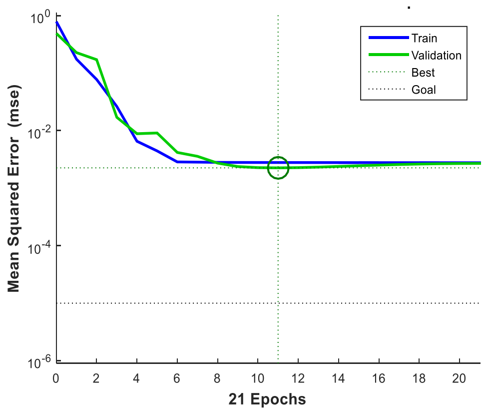

Fig. 3: Performance plot of NN-2

Based on the Levenberg-Marquardt training function (trainlm), training will stop when one of the six following conditions i.e. *Epoch, Performance Goal, Gradient, Mu, Validation Checks, Time* occur. When reached the minimum MSE validation, training will still take place to determine whether the value of MSE can still be reduced or not. If, in this case, in the subsequent epoch ten times failed to lower the MSE and fifth termination conditions (Epoch, Performance Goal, Gradient, Mu, Time) has not been reached, then the training will cease with the termination condition in the form of validation checks or max_fail reached. It can be seen in Figure 4. The weight saved networks refers to the weight of the current minimum MSE valuable validation or in this case during the training reaches epoch-11. This is the reason why the weighting NN used is based on the MSE validation not MSE training.

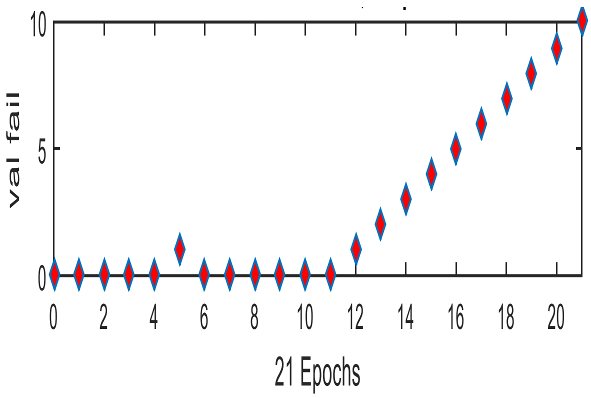

Fig. 4: Training state plot

The next step that needs to be done to evaluate the results of training the neural network is to plot the regression of training and validation. Regression plot shows the relationship between the output value (produced by the network) and target. Figure 5 below shows regression plot of training and validation result of NN-2. The correlation coefficient of training and validation result respectively are above 0.99. It indicates a good relationship between the target value and the output value (produced by the network).

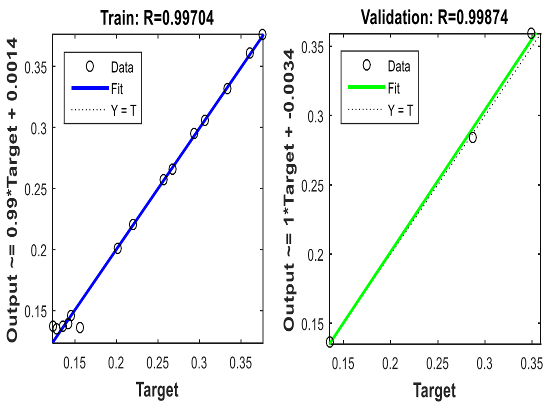

Fig. 5: Regression plot training and validation of NN-2

Test result of the selected network new input data which were obtained from EDX results, and density measurement of AAC . MSE plot based training and validation NN shown in Figure 3, it appears that the curve validation and training nearly coincident. This shows that the NN has a pretty good generalization. This generalization is related to the ability of NN predictions when given new input data that is not part of the training data.

Table 7: Comparison between predicted value and measurement value of thermal conductivity of AAC samples

Sample	Target	Prediction
AAC-1	0,214	0,243
AAC-2	0,212	0,290
AAC-3	0,214	0,320
AAC-4	0,214	0,320

Discussion:

Effect of Si, Ca Al composition and density variation on thermal conductivity of AAC , Si, Ca and Al are 3 major elements in AAC. These three elements affect the formation of dominant phase in AAC, i.e. calcium silicate hydrate (C-S-H). In addition, the density is also known to affect the thermal conductivity of AAC. Based on this information, we did simulations to investigate the influence of variations in composition of Si, Ca, Al, and the density on thermal conductivity of AAC. Simulations was conducted using NN-2.

Effect of Si composition on thermal conductivity, Figure 6. shows the relationship between the thermal conductivity of AAC and compositional variation of Si. It appears that the greater the amount of Si in AAC, the greater the thermal conductivity. It has to do with quartz - SiO_2 content of quartz in AAC since quartz is one of main constituent of AAC. Matrix phase in AAC is dominated by calcium silicate hydrate (C-S-H), in particular tober morite. During autoclaving process, it is very likely that there are small amount of unreacted SiO_2 that is resulting in residual quartz (SiO2).

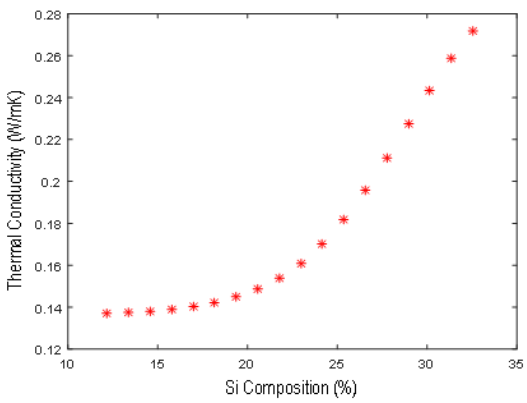

Fig. 6: Relation between thermal conductivity and Ca composition

Table 8: Thermal Conductivity of AAC , Struharova, A.,(2016).

Mineral	Thermal conductivity (W/mK)
Quartz (single crystal)	7,2 – 13,6
Tobermorite	0,18 – 0,2

Quartz has a very high thermal conductivity, i.e. 35 times greater than that of AAC in general as can be seen from Table 8 above. Therefore, to produce AAC with low thermal conductivity, Yang,R.,at.al. (2011. one thing to notice is to keep the amount residual quartz contained in the matrix phase as low as possible. This can be done by considering the composition ratio of cement and sand. Other way to reduce the amount of residual quartz in matrix phase of AAC is by using more reactive raw material than silica so that it can be more easily reacted during autoclaving process. To determine the maximum amount of Si in AAC, we calculate the value of *Vf* using equation (3). *Vf* represents volume fraction of air in AAC. Based on the results of simulation, the amount of Si in AAC should be no greater than 26.57%, since the value of *Vf* will be negative if Si amount exceed this value. Straube,B.and H. Walther, (2013.

Effect of Ca composition on thermal conductivity, Wakili,K., et.al. (2015). Existence of Ca element is associated with CaO content in AAC. CaO is one of the main constituents of calcium silicate hydrate (C-S-H) aside from SiO_2 and H_2O. Based on simulation results, shown in Figure 7, and calculation of *Vf* using Equation 3, it is found that the amount of Ca in AAC should be in the range of 22.32% to 30.35%. Beyond this range, *Vf* is negative which is not allowed

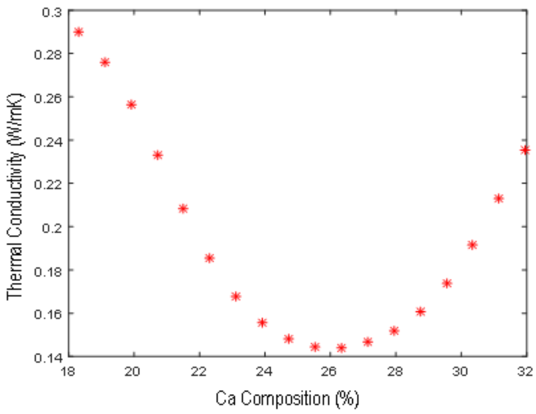

Fig. 7: Relation between thermal conductivity and Ca composition

Effect of Al composition on thermal conductivity, In contrast, with the contribution of silica that causes an increase in thermal conductivity of AAC, increasing of Al amount in AAC will lower the thermal conductivity of AAC as can be seen in Figure 8 below. One of the factors that affect the amount of Al in AAC is the use of aluminum powder as pore foaming agent. The more pore foaming agent is added, the more pores are generated so that the density of AAC was decreased. The decrease in density lead to decrease in thermal conductivity. These results are supported by previous research in [15] which shows that the thermal conductivity decreases with increasing doses of aluminum powder during the process of mixing of raw materials.

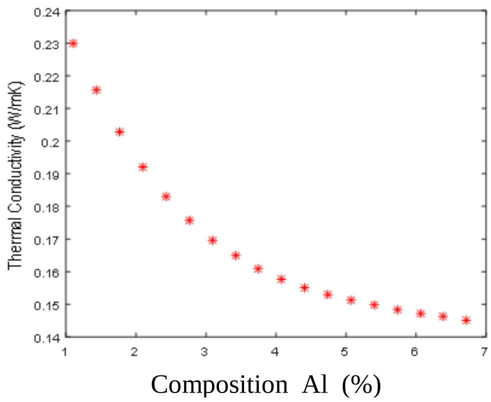

Fig. 8: Relation between thermal conductivity and Al composition

Based on the calculation of *Vf* using equation (3), it was found that minimum amount of Al contained in AAC is 2.10%. Below this value, *Vf* is negative which is not allowed. Effect of density variation on thermal conductivity, AAC with lower mass typically have greater porosity and thus lower density than that which has greater mass. Porosity of AAC directly influenced its thermal conductivity since air has lower thermal conductivity than that of solid constituent of AAC such as such as quartz, tobermorite, and C-S-H. Typical way to obtain AAC with lower density is by incorporating pore foaming agent.

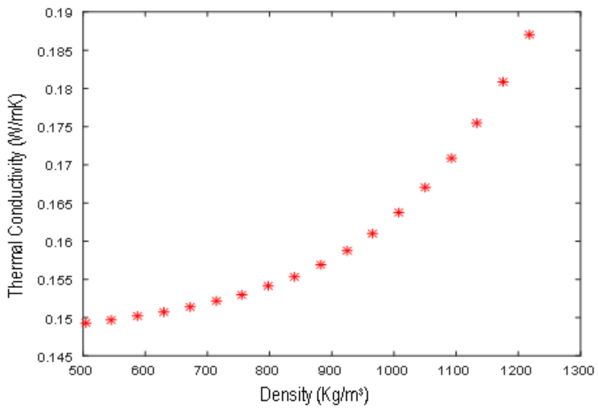

Fig. 9: Relation between thermal conductivity and density

Conclusion:

Based on training and evaluation that has been conducted on 30 network models with a variety of hidden node and weighs, it is obtained that neural network with 3 hidden node has the best performance with the following characteristics: a) the average MSE validation for 3 times of training is 0.003269, b) JST-2 has the smalles MSE validation value among the three network with three hidden node: MSE = 0.002252.

The result of testing to predict thermal conductivity of four AAC sample are as follow: AAC-1 thermal conductivity of 0.243 W / mK, the thermal conductivity of AAC-2 of 0.29 W / mK, the thermal conductivity of AAC-3 of 0.32 W / mK, the thermal conductivity of AAC-4 at 0.32 W / Mk.

Neural network simulation suggest that the amount of Si in AAC should be no greater than 26.57%, amount of Ca should be in the range of 20.32% - 30.35%, and the minimum amount of aluminum is 2.10%.

REFERENCES

1. Struharova, A., 2016. "Measuring the Thermo-technical Parameters of Autoclaved Aerated Concrete," Applied Mechanics and Materials, 824: 100-107.
2. Narayanan, N. and K. Ramamurthy, 2000. "Structure and properties of aerated concrete: a review," Cement & Concrete Composites, 22: 321-329.
3. Wakili, K., E. Hugi, L. Karvonen, P. Schnewlin and F. Winnefeld, 2015. "Thermal behaviour of autoclaved aerated concrete exposed to fire," Cement & Concrete Composites, 62: 52-58.
4. Siang, J., 2009. Jaringan Syaraf Tiruan dan Pemrogramannya menggunakan Matlab Edisi 2, Yogyakarta: Andi Yogyakarta.
5. Bal, L. and F. Bodin, 2013. "Artificial neural network for predicting drying shrinkage of concrete," Construction and Building Materials, 38: 248-254.
6. Lee, J., J. Lee and C.B.S., 2012. "Effective Prediction of Thermal Conductivity of Concrete Using Neural Network Method," International Journal of Concrete Structures and Materials, 6(3): 177-186.
7. Singh, R., R. Bhoopal and S. Kumar, 2011. "Prediction of effective thermal conductivity of moist porous materials using artificial neural network approach," Building and Environment, 46: 2063-2068.
8. Baspinar, M., I. Demir, E. Kahraman and G.G., 2014. "Utilization Potential of Fly Ash together with Silica Fume in Autoclaved Aerated Concrete Production," KSCE Journal of Civil Engineering, 18(I): 47-52.
9. Kuramaa, H., I. Topcub and C. Karakurt, 2009. "Properties of the autoclaved aerated concrete produced from Coal Bottom Ash," journal of materials processing technology, 209: 767-773.
10. Kunchariyakun, K., S. Asavapisit and K. Sombatsompop, 2015. "Properties of autoclaved aerated concrete incorporating rice husk ash as partial replacement for fine aggregate," Cement & Concrete Composites, 55: 11-16.
11. Bergman, D.L., A.S. Lavine, F.P. Incropera and D.P. Dewitt, 2011. "Apendix A: Thermophysical Properties of Matter," in Fundamental of Heat and Mass Transfer, John Wiley & Sons, Inc, p: 995.
12. Straube, B. and H. Walther, "AAC with Low Thermal Conductivity," Xella Technologie, Kloster Lehnin.
13. Grutzeck, M., 2005. "Cellular Concrete," in Cellular Ceramics: Structure, Manufacturing, Properties, and Application, Weinheim, Wiley, pp: 193-221.
14. Straube, B. and H. Walther, "AAC with Low Thermal Conductivity," Xella Technologie, Kloster Lehnin.

15. Yang, R., J. Zhu, Z. Wu, Z. Wu, M. Li and C. Peng, 2011. "Thermal Insulation and Strength of Autoclaved Light Concrete," Journal of Wuhan University of Technology-Mater. Sci. Ed., 26(I): 132-136.
16. *Zulkifli*, *Dyah Sawitri,* 2015. *Detak Yan Pratama* Optimalisation Mechanics properties ceramic High Alumina" with Ratio Komposition effect of Additive based neural network, Riset BOPTN, pp: 1-83.
17. Ali Musyafa, Yerri Susatio, Zulkifli, R. Setiyawan, 2014, "Leakage Current Test at Household Refrigerator Type Urg-129 Base Standard Nasional Indonesia (Sni) 04-6292.2.24-2001 For Safety Equipment", Asian Journal of Natural & Applied Sciences Vol. 3(4) December.pp.23-34.
18. Ali Musyafa, Faisal W.,Ya'Umar, Heri Justiono, 2015. "Heating Test at Household Refrigerator Type URG-129 Base Standard Nasional Indonesia (SNI) 04-6292.2.24-2001 for Safety Requirement" Asian Journal of Natural & Applied Sciences Vol. 4(2) June 2015, pp.24-33.